Article title: Scintillate: an open-source graphical viewer for time-series calcium imaging evaluation and pre-processing.

Journal title: Journal of Neuroscience Methods
Corresponding author: Dr. Ian Dublon
First author: Dr. Ian Dublon
Final version published online: 5-SEP-2016
Full bibliographic details: Journal of Neuroscience Methods (2016), pp. 120-127
DOI information: 10.1016/j.jneumeth.2016.08.010

Highlights

• Matlab-based graphical user interface for evaluating time-series image kinetics. • Allows whole matrix, frame-by-frame pixel change comparisons. • User may perform ICA to separate independent signals from the time series. • User may perform pre-stimulus background subtraction and additional image processing. • Open-source. Deployable on Windows and macOS as a stand-alone application.

Scintillate: An open-source graphical viewer for time-series calcium imaging evaluation and pre-processing

I.A.N. Dublon[a,□] ian.dublon@slu.se ian.dublon@gmail.com

M. Nilsson[b] A. Balkenius[a] P. Anderson[a] M.C. Larsson[a] [a]Division of Chemical Ecology, Department of Plant Protection Biology, Swedish University of Agricultural Sciences, P.O. Box 102, SE-230 53, Alnarp, Sweden [b]Lund University Bioimaging Center, Faculty of Medicine, Lund University, Lund, Sweden □Corresponding author.

Abstract

Background

Calcium imaging is based on the detection of minute signal changes in an image time-series encompassing pre- and post-stimuli. Depending on the function of the elicited response, change may be pronounced, as in the case of a genetically encoded calcium-reporter protein, or subtle, as is the case in a bath-applied dye system. Large datasets are thus often acquired and appraised only during post- processing where specific Regions of Interest (ROIs) are examined.

New method

The scintillate software provides a platform allowing for near instantaneous viewing of time-sequenced tiffs within a discrete GUI environment. Whole sequences may be evaluated. In its simplest form scintillate provides change in florescence (ΔF) across the entire tiff image matrix. Evaluating image intensity level differences across the whole image allows the user to rapidly establish the value of the preparation, without a priori ROI-selection. Additionally, an implementation of Independent Component Analysis (ICA) provides additional rapid insights into areas of signal change.

Results

We imaged transgenic flies expressing Calcium-sensitive reporter proteins within projection neurons and moth mushroom bodies stained with a Ca^{2+} sensitive bath-applied dye. Instantaneous pre- stimulation background subtraction allowed us to appraise strong genetically encoded neuronal Ca^{2+} responses in flies and weaker, less apparent, responses within moth mushroom bodies.

Comparison with existing methods

At the time of acquisition, whole matrix ΔF analysis alongside ICA is ordinarily not performed. We found it invaluable, minimising time spent with unresponsive samples, and assisting in optimisation of subsequent acquisitions.

Conclusions

We provide a multi-platform open-source system to evaluate time-series images.

Abbreviations: ΔF, change of intensity between frames; ICA, independent component analysis

Keywords: optical imaging; Fluorescence; Pre-processing; Calcium imaging; ICA; GUI

1 Introduction

Calcium ions generate useful intracellular signals and control key functions in all types of neurons. Neuronal imaging of calcium is particularly important because calcium signals exert their highly specific functions in well-defined cellular sub compartments (Grienberger and Konnerth, 2012). This technique was developed in the 1960s (Shimomura et al., 1962; Ashley and Ridgway, 1968) and allows for real-time examination of neuronal potentials. Used extensively in mammalian tissue and more recently in insects (from 1999 onwards in Bees (Galizia et al., 1999) and a short while later in flies (Fiala et al., 2002), ants (Dupuy et al., 2010)) and crustaceans (Stein et al., 2011) it provides an established method to examine in-vivo excitation in relation to defined stimuli.

Recent advances in fluorescent microscopy have allowed for acquisition of functionally useful high-resolution time-series image stacks with associated change of fluorescence brought about by changes in the concentration of Ca^{2+} ions. When dealing with conventional two-dimensional fixed Z axis images, it is easy to amass vast amounts of time-sequence data and this issue is compounded for 3d images taken with variable Z depth or acquired using dedicated multi-photon imaging systems. Capturing the pre-stimulus baseline over several frames, stimulus and resulting stimulus decay creates a multiple frame .tiff that may be not insubstantial in file size. For example, a 16-bit depth unbinned, unchipped, 1024 × 1344 tiff image of 40 frames produces a resulting .tiff of 110.2 MB. Though fast storage cost has decreased substantially, advances in microprocessor technology make initial pre-processing effortless, allowing for a rapid evaluation of the preparation.

When acquiring monochromatic calcium imaging data, the user must optimise light conditions, wavelength, stimulus delivery and interval and a host of additional preparation specific parameters. Once this is done the limitation often becomes the preparation itself and its decreasing viability as time progresses. It is also common to have preparations with basal fluorescence that appear as is expected but which simply do not respond at the outset perhaps due to unintended damage to respective parts, during viewing or preparation for viewing. For example, when in-vivo imaging insect brain areas such as fluorescent Drosophila melanogaster antennal lobes containing site directed expression of Calcium sensitive fluorescent protein in projection neurons (PNs), damage to the antennal nerve frequently results in a subject displaying strong basal fluorescence but one that lacks the requisite PN antennal lobe response. In such cases acquisition of additional recordings becomes unnecessary and is also costly in terms of lamp and microscope time and storage. It is thus imperative to rapidly sacrifice the preparation and prepare anew.

In bath-applied systems where a dye is activated using monochromatic light the signal may be very weak depending on correspondingly high background fluorescence. In the moth antennal lobe, the strongest elicited response is around a 1% increase and such responses are further reduced in other brain parts such as the mushroom body (Balkenius et al., 2015). Preparation bleaching also further hinders analysis of signal change.

1.1 A priori selection in pre- and post-processing

Historically, due to limitations in computational processing power, when imaging a live subject, it is normal to pre-select areas that are likely to respond and using background information derived from literature or experience, omit areas that are considered to be irrelevant. For example, in insects when testing pheromone response in the male antennal lobe, it is normal to select regions of interest (ROIs) based on mapping obtained via previous immunohistocytochemistry (Berg et al., 1998) that encompass the macroglomerular complex. ROIs are defined during acquisition and pre-processing and kinetics evaluated through the time-series for these specific areas. This process may be logical where it minimises computational time, or where specific noisy regions such as those caused by autonomic movement must be omitted. It is however possible that additional response occurs over multiple areas that perhaps fall outside of said predefined ROIs. Assuming computational power is sufficient, it becomes trivial to examine change throughout the entire tiff matrix, for every frame.

1.2 Selection, but only after pre-processing in the first instance

Scintillate.m is a free open-source Matlab script that provides a suite of pre-processing image tools. It is designed from the outset to be compiled into a platform independent discrete application running alongside bespoke image acquisition software. It allows

the microscope operator to rapidly gauge the value of the sample being viewed, assessing the viability of the preparation in seconds, sparing microscope time, lamp hours and reducing distress to the subject. Whilst in large images, viewing pixel-by-pixel change is processor intensive, it is in our opinion preferential to accumulation and storage of further data collected from unresponsive, non-viable preparations. It also helps to ensure that any unexpected, but real signal changes are discovered. Scintillate is not intended to replace pre- or post-processing environments but is instead designed to complement existing acquisition and pre-processing systems. Its use is envisaged whilst image acquisition is on-going providing the user with signal change information and the means to further refine subsequent acquisitions. For example, once signal change has been pinpointed, the user may centre the image over that specific area, change objectives, alter camera settings such as sensor binning or simply adjust ROIs in the acquisition software.

Recent programmatic advances have allowed proprietary acquisition systems to provide substantial pre-processing tools. These however are often bound to a specific computer package necessitating substantial financial outlay. By working with stacked tiffs, this software is compatible with numerous acquisition platforms and operating systems.

1.3 Independent component analysis (ICA) with scintillate

Scintillate uses Independent Component Analysis (Comon 1994; Hyvärinen and Oja, 2000) to provide blind source separation of mixed signals which are subsequently false-colour coded.

ICA defines a generative model for observed multivariate data. Data variables are assumed to be linear mixtures of unknown latent variables, with a mixing system that is also unknown. Components are assumed to be non- gaussian and mutually independent (hence independent components). These independent components, also called sources or factors, can be determined by ICA (Hyvärinen et al., 2000). Thus, after specifying comparatively few parameters the user is able to blind-source separate signals within images and thus assign false colour coding to areas of signal change. This is done rapidly, across the entire image matrix and is designed to eliminate possible sources of pre-selection bias.

Previously ICA has been made available to Matlab via the open source FastICA toolkit (http://research.ics.aalto.fi/ica/software.shtml) and has thus far been developed into a Matlab command line toolkit, CellSort (Mukamel et al., 2009). Here we utilise the FastICA toolkit to provide ICA as a user configurable option within our GUI providing it as one option alongside additional visualisation tools. ICA has previously been used extensively in functional MRI of the human brain (Calhoun et al., 2001) and suggested, for example, as a means for presurgical mapping of the sensorimotor cortex (Mannfolk et al., 2011).

ICA is provided as part of a suite of rapid tiff inspection tools including more traditional whole matrix ΔF analysis tools, averaged pre-stimulation background subtraction, thresholding and rudimentary cropping and export tools. The user is able to work through each frame and visualise each frame as required.

2 Materials and Methods

2.1 Scintillate script

Scintillate is a platform independent Matlab .m file (available under creative common licence from https://github.com/dublon/scintillate) compatible with Matlab 8.4 (R2014b) and above utilising several functions from the Matlab Image Processing Toolbox and two from the Statistics and Machine Learning Toolbox. Moreover, if the Matlab compiler toolbox is present on the development machine, it is deployable as a standalone executable. This allows a small self-contained application (with some user installed runtime libraries) to be built enabling use of all functions on a microscopy workstation without having a Matlab installation present. Thus far it has been successfully compiled on Windows and macOS (formerly OS X) systems.

Scintillate accepts data in the form of a stacked .tiff, a common file output format for many imaging systems. The user is presented with a GUI window, menu and dialog driven interface elements alongside a panel of buttons (Fig. 1). The software is self-contained and assumes that the user has no familiarisation with Matlab or the command line making it usable by both programmers and by image acquisition personnel. As source code and the associated Matlab GUIDE .fig file is provided it can form a readily editable framework that may easily be expanded upon and developed to suit the specific needs of the imager, for example, to implement additional image formats if needed. Indeed, it is hoped that further changes to this software source code can be added as they are developed.

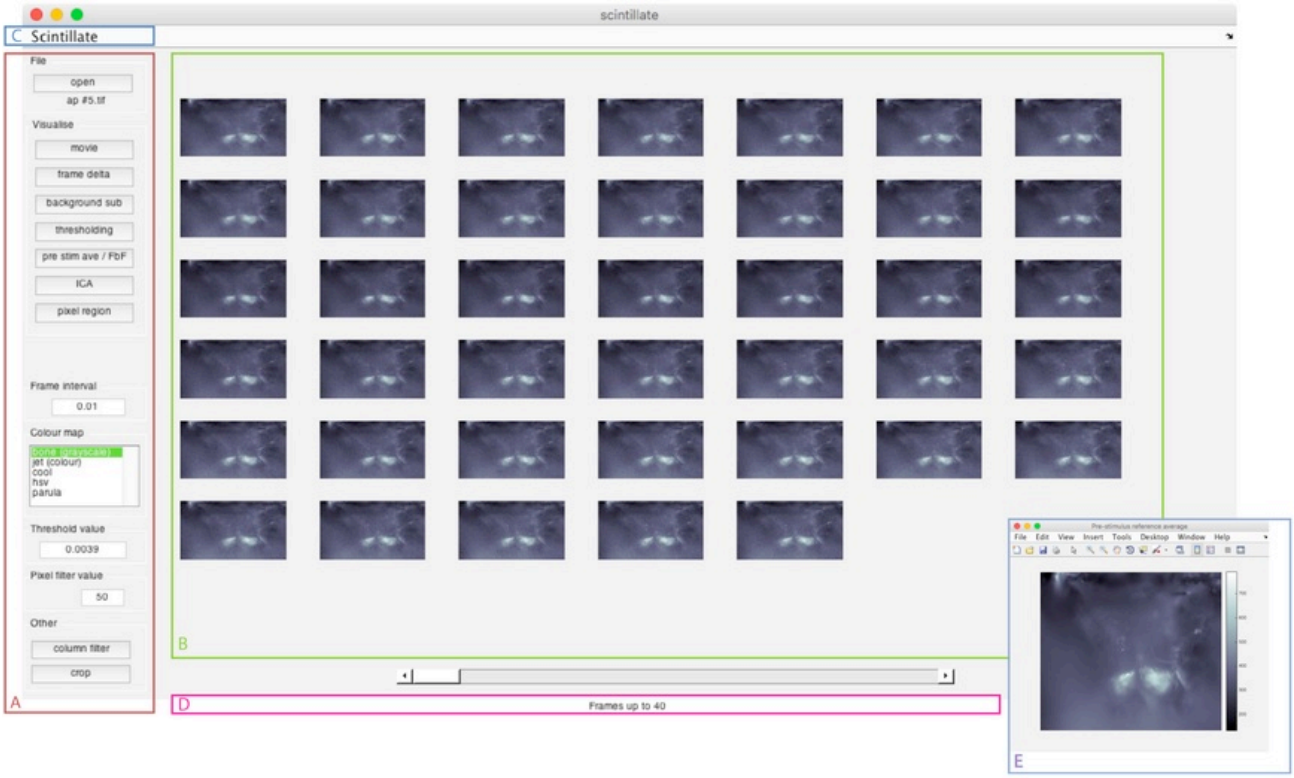

Fig. 1 Interface elements. On the left are a series of buttons instigating subfunctions (Outline A). The time-series dataset may be viewed on the main plot figure axis (Outline B). A global menu exists within the window (Outline C). Status text is updated at the base of the window (Outline D). An average of pre-stimulation frame signal is presented as a resizable graphic in its own window. Here shown at a reduced size (Outline E).

In its present form the user is able to instantly view the stacked tiff and thumbnails of each frame across time, view pre-stimulus average, subtract the pre-stimulus average from the post-stimulus frames, perform simple thresholding, pixel filtering and most usefully perform rapid ICA. The user is able to crop the image and export as a stacked .tiff that may, if required be re-read into scintillate directly. Details for these parts are presented under Theory/Calculation.

3 Experimental

Calcium imaging was conducted on mushroom bodies of Manduca sexta moths and on transgenic Drosophila melanogaster flies expressing Calcium sensitive reporter proteins in the projection neurons. F1 flies (y[1] w[1118]; P{w[+m*] = GawB}GH146/GCamP3.0; +/+) of a y[1] w[1118]; UAS-GCamP3.0; + (kindly provided by Dr S. Sachse, Max Planck Institute for Chemical Ecology, Jena) × y[1] w[1118]; P{w[+m*] = GawB}GH146 (30026, Bloomington Stock Centre, Indiana, USA) were visualised on an Olympus BX Series compound microscope (Olympus Europa SE & CO. KG, Stockholm) using 470 nm monochromatic light (PolychromeV, TillPhotonics FEI, Munich). Image acquisition was conducted with a Hamamatsu Orca R2 C10600-10B (Hamamatsu Photonics K.K., Hamamatsu, Japan) camera acquiring at 16-bit depth with, 200 ms between frames and at normal scan speed.

See Appendix A for details on insect rearing, subject preparation and stimulus delivery.

4 Theory/calculation 4.1 Live insect observations

4.1.1 *D. melanogaster*

We expected to observe strong and defined signal in response to banana and apple odour in specific sets of glomeruli. Antennal lobe glomeruli DM2 (Wong et al., 2002), DL1 (Wong et al., 2002; Marin et al., 2002) DA2 (Wong et al., 2002) VM2 (Wong et al., 2002; Marin et al., 2002) VA1 and VL2 (Wong et al., 2002) should be visible in this transgenic fly in addition to a specific

projection neuron subset (Stocker et al., 1997; Marin et al., 2005; Jefferis et al., 2001; Wong et al., 2002; Suh et al., 2004; Shang et al., 2007).

4.1.2 *M. sexta*

We expected to observe responses within the mushroom body calyces. All individuals were recorded from the same region of the left or/and right mushroom body.

4.1.3 Scintillate script

4.1.3.1 Dependencies Scintillate uses several key functions from the Image Processing Toolbox and two functions from the Statistics and Machin Learning Toolbox: prctile.m and quantile.m. Other functions are obtained via open source solutions and are discussed below.

4.1.4 GUI elements

An accompanying Matlab GUIDE file is supplied with this software allowing GUI changes to be made visually as well as programmatically. As default some buttons are disabled until data has been loaded. Slider length is calculated using the number of frames in the stack and the handle is updated once this data is available.

4.1.5 Tiff storage

Elegant, memory efficient tiff handling is facilitated by the use of TiffStack.m, a freeware open source Tiff handler for Matlab now using Libtiff (Dylan Muir: http://www.mathworks.com/matlabcentral/fileexchange/downloads/63732) also utilised in Muir and Björn (2015). Tiffs are read in to memory using this function, and made available to all functions using guidata and a status text handle is updated and displayed when this process is complete.

4.1.6 Tiff overview

Upon opening the file, the user is asked as to which frame the stimulus was presented. An average of all frames prior to stimulus is calculated and presented in a separate window alongside subplots of subsequent frames in the stack.

4.1.7 Tiff viewing

Tiff stacks are visualised using the Image processing toolbox imagesc.m function contained within a loop called by a button or the slider, with the slider handle being updated according to the correct position in the stack. Frames may be viewed according to Matlab's pre-defined colour schemes, which are user selectable via the text input box on the side (Fig. 1(A)). Frame interval can also be adjusted in a similar fashion, controlling the speed of iterations through the loop.

4.1.8 Delta up/down

Pixel-by-pixel changes in fluorescence are calculated for each pixel by producing the absolute pixel difference between the present frame and the previous frame. This is done using imabsdiff.m and compares each element in array Y (the present frame) with the corresponding element in array X (the past frame) or vice versa. This is outputted as the loop is executed. Frame rate is also user definable.

4.1.9 Column filtering

A user definable pixel filter may be applied to the image. This utilises the Matlab Image Processing Toolbox inbuilt column filter colfilt.m function where column dimensions and filter size can be specified via an input dialog and text box respectively.

4.1.10 Background pre-stimulus subtraction

Scintillate provides background pre-stimulus subtraction by calculating the pre-stimulus average and simply subtracting this image from the subsequent post-stimulus frames in the stack. A prompt is generated to ascertain at which frame the stimulus

arrives at and a composite average of the pre-stimulus frames is subtracted from each successive frame.

4.1.11 FastICA

Independent component analysis is made possible by the use of FastICA (Gävert et al., 2005 (http://research.ics.aalto.fi/ica/software.shtml)). Here we provide an initial dialog box where the user is able to enter arguments for the ICA. The user can specify downsampling level, colour emphasis and background weighting or simply accept the default values as an initial starting point. This provides for rapid ICA and subsequent refinement eliminating the need for command line syntax. Matlab's default print button has been substituted with the printpreview function allowing for additional customisation of publication ready .pdf output.

The smooth.m function dependency, ordinarily satisfied if the Curve Fitting Toolbox is present, is here substituted by the use of the open-source fastsmooth.m (Tom O'Haver: http://www.mathworks.com/matlabcentral/fileexchange/19998-fast-smoothing-function).

4.1.12 Thresholding

Thresholding is achieved where the image is first converted to 4-bit image and utilising the values of the pixel filter and the thresholding value, a simplified region is displayed. If the user provides no threshold value it is auto calculated using Otsu's method (Otsu, 1979). This value can be user adjusted in real time.

4.1.13 Cropping and stacked TIFF export

The user is able to graphically select a region of high value to crop. The output is saved as a tiff stack using the freeware Tifflib compatible saveastiff.m (YoonOh Tak: http://www.mathworks.com/matlabcentral/fileexchange/35684) and the Tiff function for each frame in the tiff stack. Using saveastiff.m provides a comprehensive set of user definable options for export that are easily configured.

4.1.14 Point by point magnification

Here we use the Image processing toolbox impixelregion.m function. This provides a panel with the selected part of the tiff in higher magnification.

5 Results

We provide three examples of processed output from our script. Please see online materials for supporting stacked tiffs.

5.1 *Drosophila*

Here we show a relatively grainy image of y[1] w[1118]; P{w[+m*] = GawB}GH146-Gal4/GCamP3.0; +/+ reared on banana and presented with a known banana stimulus (Fig. 2). We show the same fly presented with a previously un-encountered apple odour stimulus (Fig. 3) in order to display expected alternative glomerular activity. The fly preparation took around 40 min. Scintillate easily separates out signal changes in respective glomeruli. We illustrate a pronounced change in fluorescence in differing glomeruli given an alternate odour stimulus.

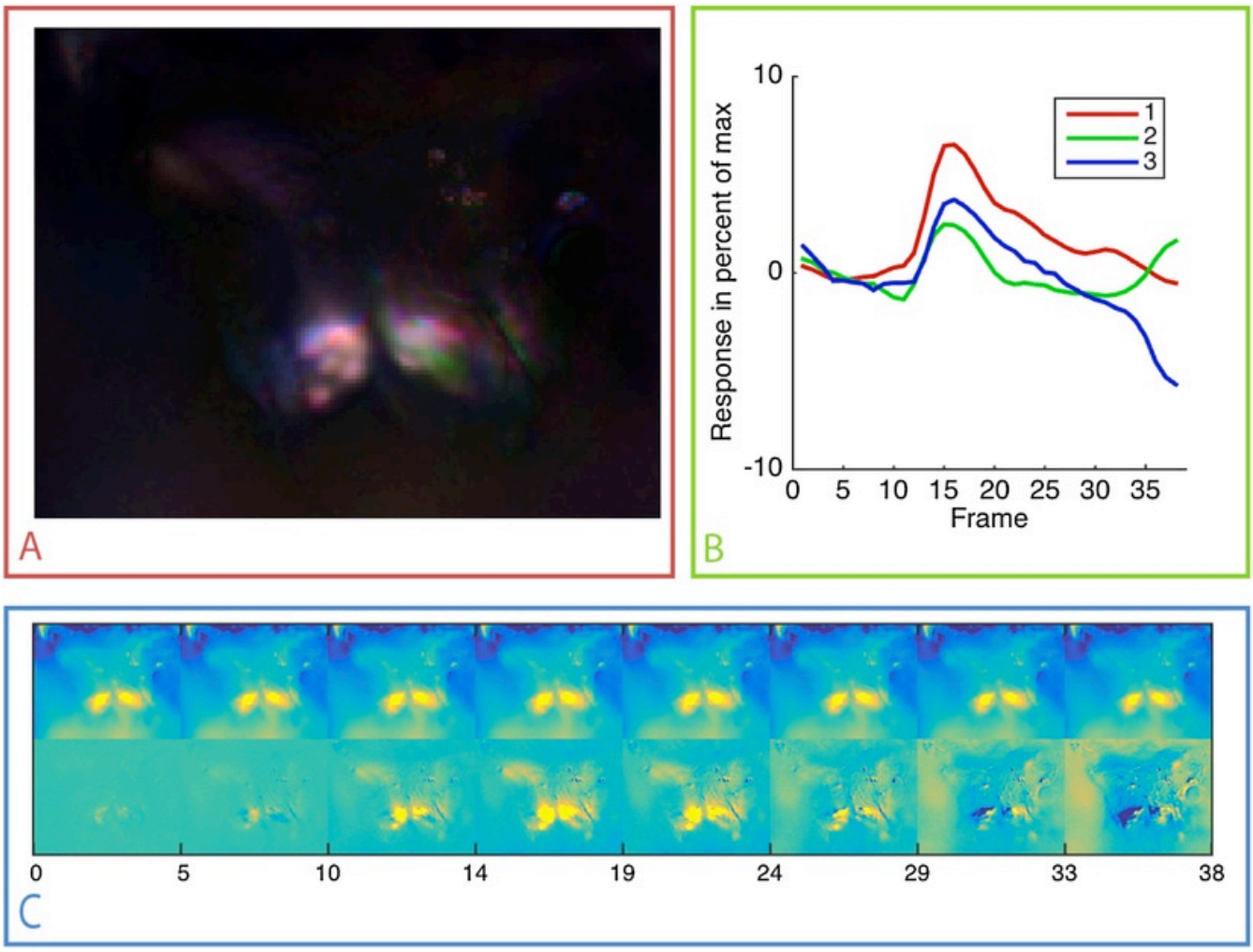

Fig. 2 Fly preparation exposed to banana odour at frame 11, ICA produced in the default mode (downsampled to 150px). This is direct scintillate output as a high-resolution .pdf though shown here with overlaid added annotations. Panel A shows false colou coded image relating to ICA components. Panel B shows the three most pronounced independent components, and provides an overview of how the signal changes over time. Panel C shows snapshots of the input images for selected frames at the top, and th pre-processed images used for the ICA analysis at the bottom.

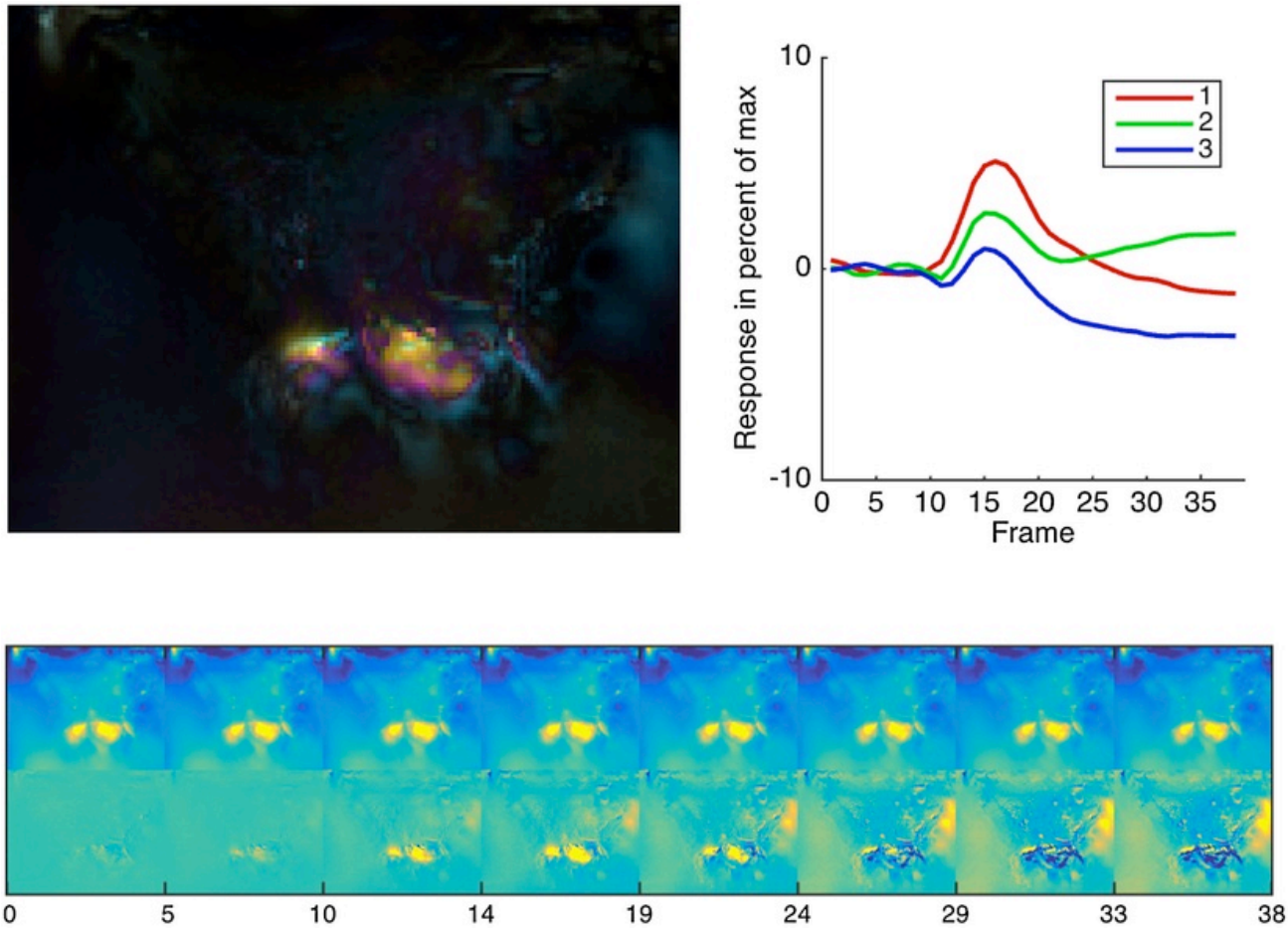

Fig. 3 The same fly as in Fig. 2, here exposed to apple odour for the first time at frame 11, ICA produced in the default mode (downsampled to 150px). This is direct scintillate output as a high-resolution .pdf.

5.2 *Manduca*

Here we successfully show a very slight change that would otherwise be difficult to determine at the acquisition stage. The influence of vision was seen in the same regions that reacted to olfactory stimuli (Fig. 4).

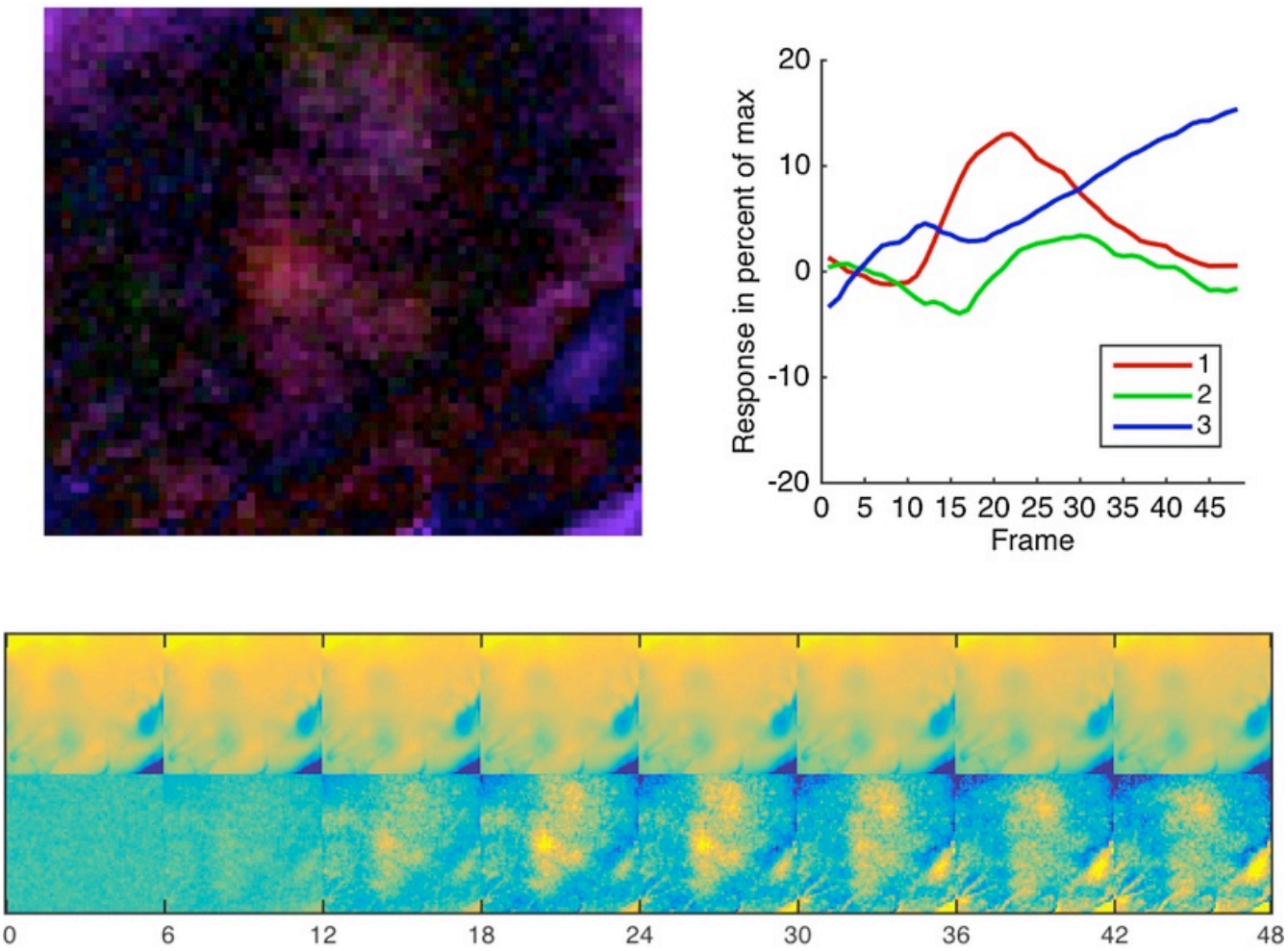

Fig. 4 Moth preparation exposed to bergamot and light stimulation. Here the third ICA component probably shows motion where the blue pixels are situated at the edges of the sample. (For interpretation of the references to colour in this figure legend, the reader is referred to the web version of this article.)

6 Discussion and conclusions

In preparations where signal response is weak it is imperative to examine the whole image without pre-selection bias. Often evoked response is clearly defined and restricted to certain and expected areas; however, this may not always be the case.

In cases where basal fluorescence is present but where the subject does not respond at all due to damage it is all too easy to lose time making recordings. This is both disheartening for the researcher and potentially distressing for the preparation. Whilst obtaining a perfect dissection is always the objective, it may be possible to reduce preparation time in return for more frequent preparation viability. Assessing preparation viability is made much easier by using the scintillate software. Performing in-vivo imaging in a fruitfly requires considerable dissection care. Preparations, however good, are likely to be variable in quality (Grabe et al., 2014).

Where autonomic movement is observed it is possible to observe erroneous activation patterns along the edges of an activation region where motion and activation time courses are conflated. Resolving this is not easy though assuming the activated areas are substantially larger than the scope of the motion and the movement is clearly occurring in the periphery it may be possible to exclude such areas by cropping. Generally, if substantial movement is present it may, where possible necessitate further fixation or a new preparation. Movement remains a key issue when imaging insects (Kain et al., 2016).

ICA provides a simple and effective method of identifying areas of signal change and this method combined with ΔF across each pixel makes scintillate an eminently useful tool for any person performing calcium imaging.

Author contributions

Wrote the software: IAND and MN. Devised the experiment IAND, PA, and ML (flies), AB (moths). Performed the experiment IAND (flies) and AB (moths). Wrote the manuscript: IAND, MN, AB, PA and ML. Edited the manuscript: all authors. All authors have read and approved the manuscript prior to submission. We know of no competing interests.

Acknowledgements

This project was supported by postdoctoral funding to IAND from SLU's Lighthouse Project on Spodoptera littoralis host search. IAND would like to thank C Marcu (Alnarp IT-avdelningen). We thank Dr S Sachse for fly supply and for hosting IAND at Max Planck Institute for Chemical Ecology, Jena. We would also like to thank two anonymous peer reviewers for very helpful and constructive commentary.

Appendix A Insect rearing

The hawkmoth Manduca sexta (Lepidoptera: Sphingidae) was reared on an artificial diet (Bell and Joachim, 1976) with 200 mg/L beta-carotene added (Goyret et al., 2008). Individuals were reared under a 16:8 h light:dark cycle at 23–25 °C, 40–50% relative humidity. Experiments were performed on 2–4 days post-emergent naïve moths.

Fly lines were reared at 25° C and 60% relative humidity on a 16:8 h light:dark cycle. Individuals used in fly stock were reared on a synthetic medium based around the Bloomington stock centre's recipe 1 (http://flystocks.bio.indiana.edu/Fly_Work/media-recipes/media-recipes.htm). For data shown here flies with the required genotype were reared directly on banana itself.

Insect preparations

Individual flies were prepared for in-vivo imaging using a preparation based on the method described in Silbering et al., 2012. In summary, flies were carefully inserted into a 125 μm slot made from an opened 3.05 mm athene

alt-text: Fig. 4

grid (G220-5, Plano GmbH, Wetzlar, Germany), with the U-shaped grid forming a collar between the head and thorax. This grid was itself attached to a custom made fly holder using superglue (Loctite 401, Henkel Ltd., Hemel Hemstead, UK).

In one of three changes to Silbering et al., 2012, for fly head fixation a two-component, quick drying dental cement (3 M Espe Protemp II A1, Plusdent Aps, Copenhagen, Denmark) was used instead of roisin. This provided a rapid drying and easily removable fixture immobilising the fly. Once the fly was securely immobilised within the grid, antennae were very carefully tensioned away from the cuticular incision area using a 0.05 Ω wire, inserted behind the antennal segments. This wire was itself affixed with wax to a plastic cover slip using dental wax (Deiberit 502 Hard Sticky Wax 209212, Siladent, Goslar, Germany) melted with a warm soldering iron (Minityp S, Ersa Lötkolben elektrisch, 6 W, 12 V, Bräunlich GmbH, Lutherstadt Wittenberg, Germany). This cover slip and wire were subsequently tensioned in order to gently draw forward the antennae away from the incision area.

In a second rather more substantial change as compared to Silbering et al., 2012, instead of using an immersive lens, and thanks to the preferential optics of a modern camera, a 20× air objective (Olympus UMPlanFI 20X/0.50 W, Japan) or smaller, was used instead of a water immersive objective and no further antennal protection was used prior to opening the fly head (imaging of fly antennal lobe does not work reliably if water reaches the antennae). This enabled rapid fly preparation because there was a substantially reduced risk of antennal wetness with merely a small amount of ringer added to the open head. Whilst there is an inevitable trade-off with image quality and an increased possible risk of chromatic aberration, there is a vastly decreased preparation time due to decreased difficulty (around 30 min as opposed to 150 min) and increased viability may often compensate for this.

In the last substantial change, the fly head cuticle was opened with an electrolytically sharpened tungsten electrode mounted in a glass pipette as opposed to a stab knife. This provided an inexpensive dissection tip that could easily be discarded or re-sharpened

as necessary.

Individual moths were secured in a plastic pipette tip, with the head protruding from the narrow end and fixed by dental wax (Surgident, Heraeus Kulzer GmbH, Hanau, Germany) in methods similar to those described in the literature (Balkenius and Hansson, 2012). The head capsule was opened between the antennae and the eyes and muscle, glands, trachea neural sheath and the oesophagus were removed to expose the antennal lobes and mushroom bodies. Eyes were covered using a flexible tube connected to a light guide that was illuminated only during visual stimulus delivery.

A calcium green-2-AM dye (Molecular Probes, Eugene, USA) was dissolved in 20% Pluronic F-127 dimethyl sulfoxide (Molecular Probes, Eugene, USA) and diluted in moth Ringer solution to 30 μM. The calcium dye was applied directly to the brain and the preparation was left in a dark and cold (5–8 °C) environment for 1–2 h. Recordings were made in vivo after incubation and washing.

Stimuli

Antennae were stimulated with a directed odour stimulus delivered at frame 11. Camera and stimulus timing was synchronised via the use of a TillPhotonics Image control unit (ICU) connected to a Syntech stimulus controller (CS-55, Syntech, Hilversum, The Netherlands) and to a PC running Live Acquisition v.2.2.0 (FEI, Munich, Germany).

D. melanogaster individuals were presented with an aliquot of banana (0.3 g of crushed banana) or apple (0.3 g of crushed apple), carefully transferred into a glass Pasteur pipette. M. sexta were presented with 50 μl of bergamot odour in conjunction with a visual stimulus generated by a 3 mm LED of 430 nm and an intensity of approximately 0.01 cd m^2 (full moon intensity). This blue colour is known to

be attractive to the moths during foraging (Cutler et al., 1995). Here we used a combination of a visual and odour stimuli simply because the moths used were imaged as part of an ongoing unrelated imaging experiment. The light source was controlled by a custom-made interface box, which controlled the intensity of the visual stimulus. A fibre-optic light guide was used to transfer the visual stimulus to the eyes of the moth. The optically

isolated light guides where docked to the eyes using small rubber tubes that were kept in place using dental wax.

Appendix B. Supplementary data

Supplementary data associated with this article can be found, in the online version, at http://dx.doi.org/10.1016/j.jneumeth.2016.08.010.

References

Ashley C.C. and Ridgway E.B., Simultaneous recording of membrane potential, calcium transient and tension in single muscle fibers, Nature **219**, 1968, 1168–1169.

Balkenius A. and Hansson B.S., Discrimination training with multimodal stimuli changes activity in the mushroom body of the hawkmoth Manduca sexta, PLoS One **7** (4), 2012, e32133, http://dx.doi.org/10.1371/journal.pone.0032133.

Balkenius A., Johansson A.J. and Balkenius C., Comparing analysis methods in functional calcium imaging of the insect brain, PLoS One **10** (6), 2015, e0129614, http://dx.doi.org/10.1371/journal.pone.0129614.

Bell R.A. and Joachim F.A., Techniques for rearing laboratory colonies of tobacco hornworms and pink bollworms, Ann. Entomol. Soc. Am. **266**, 1976, 365–373.

Berg B.G., Almaas T.J., Bjaalie J.G. and Mustaparta H., The macroglomerular complex of the antennal lobe in the tobacco budworm moth Heliothis virescens : specified subdivision in four compartments according to information about biologically significant compounds, J. Comp. Physiol. A **183** (6), 1998, 669–682.

Calhoun V.D., Adali T., Pearlson G.D. and Pekar J.J., A method for making group inferences from functional MRI data using

independent component analysis, Hum. Brain Mapp. **14**, 2001, 140–151.

Comon P., Independent component analysis: a new concept?, Signal Process. **36** (3), 1994, 287–314.

Cutler D.E., Bennett R.R., Stevenson R.D. and White R.H., Feeding behavior in the nocturnal moth Manduca sexta is mediated mainly by blue receptors, but where are they located in the retina?, J. Exp. Biol. **198**, 1995, 1909–1917.

Dupuy F., Josens R., Giurfa M. and Sandoz J.-C., Calcium imaging in the ant Camponotus fellah reveals a conserved odour-similarity space in insects and mammals, BMC Neurosci. **11**, 2010, 28.

Fiala A., Spall T., Diegelmann S., Eisermann B., Sachse S., Devaud J.M., Buchner E. and Galizia C.G., Genetically expressed cameleon in Drosophila melanogaster is used to visualize olfactory information in projection neurons, Curr. Biol. **12**, 2002, 1877–1884.

Galizia C.G., Sachse S., Rappert A. and Menzel R., The glomerular code for odor representation is species specific in the honeybee Apis mellifera, Nat. Neurosci. **2**, 1999, 473–478.

Goyret J., Pfaff M., Raguso R.A. and Kelber A., Why do Manduca sexta feed from white flowers? Innate and learnt colour preferences in a hawkmoth, Naturwissenschaften **95** (6), 2008, 569–576.

Grabe V., Strutz A., Baschwitz A., Hansson B.S. and Sachse S., Digital in vivo 3D atlas of the antennal lobe of Drosophila melanogaster, J. Comp. Neurol. **523**, 2014, 530–544.

Grienberger C. and Konnerth A., Imaging calcium in neurons, Neuron **73** (5), 2012, 862–885.

Gävert H, Hurri J, Särelä J, Hyvärinen A. The FastICA MATLAB package, v2.5. (2005-10-19) http://www.cis.hut.fi/projects/ica/fastica

Hyvärinen A. and Oja E., Independent component analysis: algorithms and application, Neural Netw. **13** (4–5), 2000, 411–430.

Hyvärinen A., Karhunen J. and Oja E., Independent Component Analysis New Jersey, 2000, John Wiley & Sons, Inc., xvii.

Jefferis G.S.X.E., Marin E.C., Stocker R.F. and Luo L., Target neuron prespecification in the olfactory map of Drosophila, Nature **414** (6860), 2001, 204–208.

Kain P., Boyle S.M., Tharadra S.K., Guda T., Pham C., Dahanukar A. and Ray A., Retraction: odour receptors and neurons for DEET and new insect repellents (Nature 2013;502 : 507–512), Nature 2016, http://dx.doi.org/10.1038/nature18613, (advance online publication).

Mannfolk P., Nilsson M., Hansson H., Ståhlberg F., Fransson P., Weibull A., Svensson J., Wirestam R. and Olsrud J., Can resting-state functional MRI serve as a complement to task-based mapping of sensorimotor function? A test–retest reliability study in healthy volunteers, J. Magn. Reson. Imaging **34**, 2011, 511–517.

Marin E.C., Watts R.J., Tanaka N.K., Ito K. and Luo L., Developmentally programmed remodelling of the Drosophila olfactory circuit, Development **132** (4), 2005, 725–737. Muir D.R. and Björn K., FocusStack and StimServer: a new open source MATLAB toolchain for visual stimulation and analysis of two-photon calcium neuronal imaging data, Front. Neuroinf. **8**, 2015, 85,

Marin E.C., Jefferis G.S., Komiyama T., Zhu H., Luo L. Representation of the glomerular olfactory map in the Drosophila brain. Cell **109**(2), 2002, 243--255. http://dx.doi.org/10.3389/fninf.2014.00085.

Mukamel E.A., Nimmerjahn A. and Schnitzer M.J., Automated analysis of cellular signals from large-scale calcium imaging data, Neuron **63** (6), 2009, 747–760.

Otsu N., A threshold selection method from gray-level histograms, IEEE Trans. Syst. Man Cyber. **9** (1), 1979, 62–66, http://dx.doi.org/10.1109/TSMC.1979.4310076.

Shang Y., Claridge-Chang A., Sjulson L., Pypaert M. and Miesenbock G., Excitatory local circuits and their implications for olfactory processing in the fly antennal lobe, Cell **128** (3), 2007, 601–612.

Shimomura O., Johnson F.H. and Saiga Y., Extraction, purification and properties of aequorin, a bioluminescent protein from the luminous hydromedusan, Aequorea, J. Cell. Comp. Physiol. **59**, 1962, 223–239.

Silbering A.F., Bell R., Galizia C.G. and Benton R., Calcium imaging of odor-evoked responses in the drosophila antennal lobe, J. Vis. Exp. 2012, e2976, http://dx.doi.org/10.3791/2976. Stein W., Städele C. and Andras P., Optical imaging of neurons in the crab stomatogastric ganglion with voltage-sensitive dyes, J. Vis. Exp. 2011, e2567, http://dx.doi.org/10.3791/2567.

Stocker R.F., Heimbeck G., Gendre N. and de Belle J.S., Neuroblast ablation in Drosophila P[GAL4] lines reveals origins of olfactory interneurons, J. Neurobiol. **32** (5), 1997, 443–456.

Suh G.S.B., Wong A.M., Hergarden A.C., Wang J.W., Simon A.F., Benzer S., Axel R. and Anderson D.J., A single population of olfactory sensory neurons mediates an innate avoidance behaviour in Drosophila, Nature **431** (7010), 2004, 854–859.

Wong A.M., Wang J.W. and Axel R. Spatial representation of the glomerular map in the Drosophila protocerebrum. Cell **109**(2), 2002, 229--241.

Appendix B. Supplementary data

The following are Supplementary data to this article:

Multimedia Component 1 Multimedia Component 2 Multimedia Component 3 Multimedia Component 4 Multimedia Component 5